Dynamic Structure and Potential Energy Surface of a Three-Helix Bundle Protein

Marya Lieberman, Michael Tabet, and Tomikazu Sasaki*

Contribution from the Department of Chemistry, University of Washington, Seattle, Washington 98195

Received November 16, 1993®

Abstract: Four kinetically trapped substates of a molten globule-like artificial protein were formed by metal-directed trimerization of an amphiphilic peptide modified with a bipyridine ligand. Although the helical contents of the trapped states range from 50% to 95%, their thermodynamic stabilities are within 0.3 kcal/mol of one another. Each metalloprotein incorporates a different diastereomer of the iron(II) tris(bipyridine-peptide) core; as the diastereomers isomerize at room temperature, the four protein states interconvert, with half-lives on the order of 5 h. With the aid of a model compound, Fe(Ala-bipy)$_3$, the effects of interhelix interactions were disentangled from the effects of metal complexation, and barriers on the protein's potential energy surface were determined. The energetic barriers range from 0.5 to 1.7 kcal/mol, significantly smaller than the 2.3 kcal/mol required to unfold the metalloprotein; since the activation energy of denaturation cannot be smaller than $\Delta G°$ of denaturation, the protein does not unfold completely in the transitions from one molten globule state to another. Tertiary structure in *de novo* designed proteins is discussed in light of these results.

Introduction

The potential energy of a protein conformation depends on many factors.[1] A small change, such as the mutation of a residue, may have large energetic consequences. Other mutations leave the protein's conformation unaffected.[2] Understanding how potential energy varies with conformation is the key to predicting the folded conformations adopted by natural proteins and to designing proteins with desired tertiary structures, yet there are formidable difficulties associated with studying the potential energies of conformations of existing proteins.

A natural protein has a unique folded conformation, represented in Figure 1 as the point at the bottom of the potential well. There are other observable protein states, i.e. "unfolded" or "molten globule" states, which are believed[3] to be ensembles of conformations with similar energies. The relative energies of the ground state[4] or of an ensemble of molten globule states[5] and of the manifold of unfolded states can be determined and used to construct a crude map, such as Figure 1, of the protein's potential energy well.

The unfolded, molten globule, and native states of proteins are very different in structure. The unfolded state lacks secondary structure and is conformationally mobile. While the molten globule state retains much of the secondary structure of the folded state, it samples a large number of tertiary structures. Neither the unfolded state nor the molten globule is a singular entity; rather, both are ill-defined ensembles of conformations. The unavailability of stable intermediate states limits our ability to map the free energy surface of a protein at points other than the native state. Synthetic proteins that undergo heat- or metal-dependent transitions from a molten globule-like state to a more native-like state have been described,[6] but their molten globule states are subject to the same limitations that beset native proteins. In this paper, we describe a potentially general way to "freeze

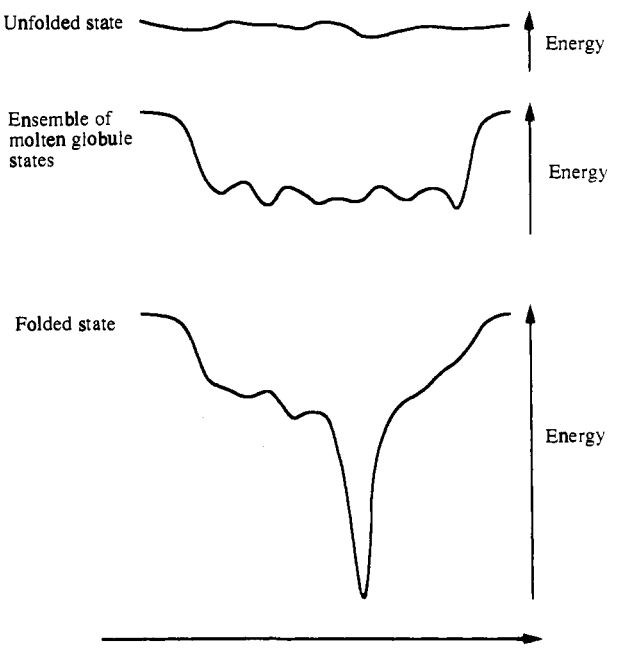

Figure 1. Potential energy well for a typical native protein, showing the unique folded state and the ensembles of molten globule and unfolded states.

* Abstract published in *Advance ACS Abstracts,* May 1, 1994.

(1) Creighton, T. E. *Proteins: Structures and Molecular Principles*; Freeman: New York, 1984.

(2) (a) Lecomte, J. T. J.; Matthews, C. R. *Protein Eng.* **1993**, *6*, 1–10. (b) Pinker, R. J.; Lin, L.; Rose, G. D.; Kallenbach, N. R. *Protein Sci.* **1993**, *2*, 1099–1105. (c) Fersht, A. R.; Matouschek, A.; Serrano, L. *J. Mol. Biol.* **1992**, *224*, 771–859. (d) Zhang, X.-J.; Baase, W. A.; Matthews, B. W. *Biochemistry* **1991**, *30*, 2012–2017.

(3) (a) Ptitsyn, O. B. *FEBS Lett.* **1991**, *285*, 176–181. (b) Kuwajima, K. *Proteins: Struct., Funct., Genet.* **1989**, *6*, 87–103. (c) Lecomte, J. T. J.; Matthews, C. R. *Prot. Eng.* **1993**, *6*, 1–10.

(4) Pace, C. N.; Shirley, B. A.; Thomson, J. A. In *Protein Structure: A Practical Approach*; Creighton, T. E., Ed.; IRL: Oxford, 1989.

(5) Molten globule states and kinetically trapped folding intermediates have been studied: (a) Handel, T. M.; Williams, S. A.; DeGrado, W. F. *Science* **1993**, *261*, 879–885, Zn-binding designed protein. (b) Baker, D.; Sohl, J. L.; Agard, D. A. *Nature* **1992**, *356*, 263–266, measured the barrier between a kinetically trapped folding intermediate and the native state as >27 kcal/mol. (c) Myer, Y. P.; MacDonald, L. H.; Verma, B. C.; Pande, A. *Biochemistry* **1980**, *19*, 199–207, horse heart ferricytochrome *c* molten globule. (d) Robson, B.; Pain, R. H. *Biochem. J.* **1976**, *155*, 331–344, penicillinase molten globule. (e) Alonso, D. O. V.; Kill, K. A.; Stigter, D. *Biopolymers* **1991**, *31*, 1631–1649, theoretical study of apomyoglobin. (f) Barrick, D.; Baldwin, R. L. *Biochemistry* **1993**, *32*, 3790–3796, apomyoglobin molten globule. (g) Barrick, D.; Baldwin, R. L. *Protein Sci.* **1993**, *2*, 869–876, apomyoglobin molten globule. (h) Nitta, K.; Tsuge, H.; Iwamoto, H. *Int. J. Pept. Protein Res.* **1993**, *41*, 118–123, lysozyme folding intermediates.

(6) (a) Handel, T. M.; Williams, S. A.; DeGrado, W. F. *Science* **1993**, *261*, 879–885. (b) Raleigh, D. P.; DeGrado, W. F. *J. Am. Chem. Soc.* **1992**, *114*, 10079–10081.

0002-7863/94/1516-5035$04.50/0

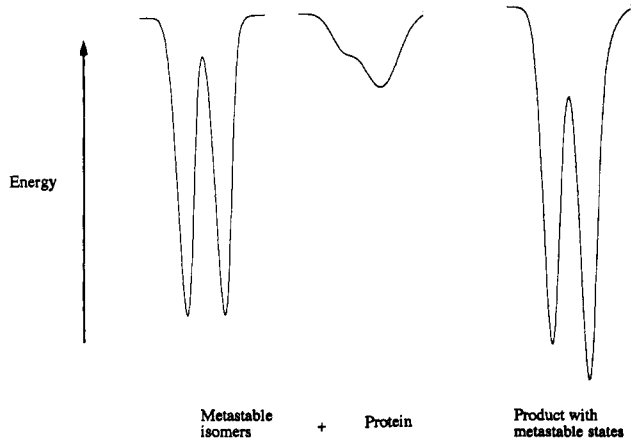

Figure 2. Superposition of a potential energy surface with metastable states, left, on a shallow protein potential energy surface, center, which results in metastable protein states. For each potential energy surface, the x-axis is a coordinate in conformational space.

out" metastable states in an artificial protein and what we have learned from this technique about the potential energy surface of a particular parallel three-helix bundle protein.

Although most proteins lack stable states other than the native state,[5] if another potential energy well with multiple stable states were superposed on a protein's potential energy well, multiple products would be formed. Figure 2 shows a schematic diagram of this approach. The potential energy well of a template molecule is shown on the left; in this example, it has two metastable configurations which may interconvert by passing over a large kinetic barrier. The potential energy well of a protein fragment that may be attached to the template is shown in the center; it lacks a single stable configuration, and the barriers to interconversion of local minima are relatively low. This protein fragment by itself would be expected to exist as an ensemble of configurations. The potential energy well on the right shows how the conformational constraints provided by the template molecule trap out observable protein states in the template–protein conjugate. By comparing the energies of the metastable states of the template–protein conjugate with those of the template molecule, we can investigate the energies of states on the protein's potential energy surface.

We have described how an amphiphilic peptide modified with bipyridine forms a three-helix bundle protein when iron is added.[7] The metal holds the helices in four different spatial arrangements. Since the binding energy of $Fe(bipy)_3$ is much larger than the energy of peptide–peptide interactions in the parallel bundle of helices, the potential well of the metal complex is not greatly perturbed by the presence of the protein, and substates that correspond to local minima in the iron tris(ligand) potential well can be isolated and characterized. By studying a model compound, $Fe(Ala\text{-}bipy)_3$, we can disentangle the effects of the two potential wells and form a picture of the potential energy surface on which the parallel three-helix bundle protein lies.

Experimental Section

Materials. *t*-BOC and FMOC amino acids, *N*-hydroxybenzotriazole, diisopropylcarbodiimide, trifluoroacetic acid, and diisopropylethylamine were purchased from Advanced ChemTech and used as received. Dicyclohexylcarbodiimide was purchased from Sigma. Dimethylformamide, dichloromethane, and HPLC-grade acetonitrile were purchased from Baker. 2,2′-Bipyridine was purchased from Aldrich and recrystallized from hexane. Thionyl chloride and 4,4′-dimethyl-2,2′-bipyridine were bought from Aldrich and used without further purification.

Instruments. pH was measured with a Radiometer Copenhagen PHM84 pH meter equipped with a microprobe. UV-vis specta were acquired on a Perkin-Elmer Lambda 3B spectrometer in 1-cm quartz semi-micro cells. HPLC was performed using a Waters 600E system, with a Perkin-Elmer LC-95 UV–vis detector, Kipp and Zonen BD-40 chart recorder, and an HP3394A integrator.

Scheme 1

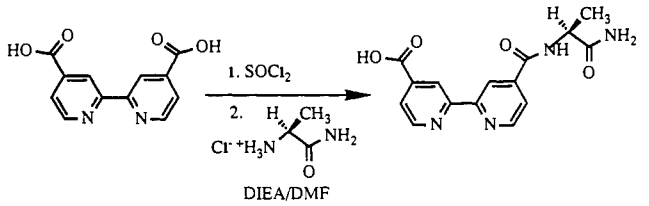

Electrospray MS. Electrospray mass spectra were acquired on a Sciex API III triple-quadrupole mass spectrometer fitted with a nebulization-assisted electrospray ionization source (PE/Sciex, Thornhill, Ontario). Lyophilized peptides were dissolved to a final concentration of approximately 1×10^{-5} M in 1:1 methanol/H_2O (v/v), 0.1% in formic acid. Samples were infused at 3 μL/min with a Harvard Apparatus pump. Positive ion MS was run with an orifice voltage of 150–200 V. Spectra were collected and analyzed using software provided by Sciex Corp.

Circular Dichroism Spectra. A JASCO-700 circular dichroism spectrometer with 0.1–2.0 mm pathlength cells and a nitrogen flow rate of 5 L/min was used to make CD measurements. Peptide concentrations ranged between 0.2 and 2 mM. The cell blank was subtracted, the spectra were smoothed, and the smoothed spectra were compared with the unsmoothed ones to make sure they were not overfiltered. The molar ellipticity per backbone amide at 222 nm was used to estimate the helical content, with 100% helicity estimated[8] at 33 500 deg mol^{-1} cm^{-2}.

Sedimentation Equilibrium Centrifugation. Sedimentation equilibrium centrifugation was done in a Beckman Spinco Airfuge using a 30-deg rotor. In a typical experiment, $Fe(pepy)_3$ was made up to 0.75 mM in 25 mM pH 4.8 acetate buffer with 10 mg/mL Dextran-6000 added to stabilize the concentration gradient. Duplicate 200-μL samples were centrifuged at an average rotor speed of 81 250 rpm. After 22 h of centrifugation, the tubes were placed upright and 10-μL fractions were removed with a syringe attached to a micromanipulator. Each fraction was diluted with 600 μL of pH 4.8 buffer, and the absorbance at 294.5 and 220 nm was measured and plotted vs $1/r^2$, where r was the average radial distance of the 10-μL sample from the center of the rotor. Apparent molecular weights were calculated from the slope of this plot, as described by Pollet et al.[9] (The apparent molecular weights of standards (standard deviation in parentheses) were as follows: Vitamin B_{12} (fw = 1350) found $1.1(2) \times 10^3$. Cytochrome *c* (fw = 12 400) found $1.2(2) \times 10^4$. Myoglobin (fw = 17 500) found $1.7(2) \times 10^4$.)

Binding Constants. Binding constants for the iron complexes of pepy, Ala-bipy, and bipy were determined spectroscopically at pH 4.8 as described.[10] The binding constant found for $Fe(bipy)_3$ at pH 4.8 was $8(3) \times 10^{16}$. Since the pK_a for bipy is 4.45,[11] the measured K_b was corrected to account for monoprotonated bipyridine that is present at pH 4.8; the calculated K_b at pH 7.0 is $2.5(1.0) \times 10^{17}$ (2.8×10^{17} lit.[12]).

Ala-bipy. 4,4′-Dicarboxy-2,2′-bipyridyl was prepared from 4,4′-dimethyl-2,2′-bipyridyl by oxidation with potassium permanganate according to the literature procedure.[13] As shown in Scheme 1, 4,4′-dicarboxy-2,2′-bipyridyl (1.40 g, 5.73 mmol) was placed into a 50-mL round-bottomed flask equipped with a magnetic stir bar and a reflux condenser fitted with a drying tube. Thionyl chloride (15 mL) was added, and the mixture was refluxed overnight. The resulting yellow solution was distilled to remove excess thionyl chloride. The residue was washed several times with hexane to remove dimethyl bipyridine. The crude diacid chloride was stirred with 10 mL of DMF at room temperature. Alanine amide·HCl (0.70 g, 5.6 mmol) was dissolved in 10 mL of DMF and treated with 4 mL of diisopropylethylamine in 5 mL of DMF. The alanine solution was added dropwise with vigorous stirring to the diacid chloride solution over a 30-min period. The yellowish solution turned light red. DMF was removed by rotary evaporation, and the mixture was lyophilized twice from water. The resulting red-brown solid was

(7) Lieberman, M.; Sasaki, T. *J. Am. Chem. Soc.* **1991**, *113*, 1470–1471.

(8) (a) Johnson, C. *Proteins: Struct., Funct., Genet.* **1990**, *7*, 205. (b) Chang, C. T.; Wu, C.-S.; Yang, J. T. *Anal. Biochem.* **1978**, *91*, 13.

(9) Pollet, R. J.; Haase, B. A.; Standaert, M. L. *J. Biol. Chem.* **1979**, *254*, 30–33.

(10) Sasaki, T.; Lieberman, M. *Tetrahedron* **1993**, *49*, 3677–3689.

(11) James, B. R.; Williams, R. J. P. *J. Chem. Soc.* **1961**, 2007.

(12) Irving, H.; Mellor, D. H. *J. Chem. Soc.* **1962**, 5222.

(13) Launikonis, A.; Lay, P. A.; Mau, A. W.-H.; Sargeson, A. M. *Aust. J. Chem.* **1986**, *39*, 1053–1062.

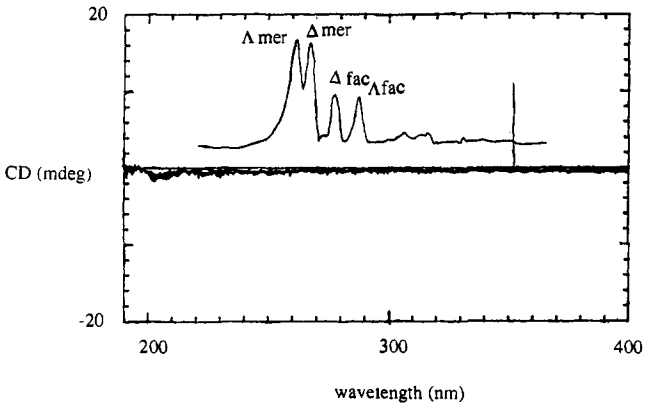

Figure 3. Unsmoothed CD spectrum of an equilibrium mixture of isomers of Fe(Ala-bipy)$_3$. [Ala-bipy] = 8.2×10^{-5}, 0.5-mm cell. Inset: HPLC trace of the same mixture.

recrystallized from 1:1 water/acetonitrile to give 0.33 g (19% yield) of white crystals. FABMS: m/z = 314, found 315 (M + H) and 337 (M + Na). UV–vis (pH 4.8 acetate): λ_{max} = 293 nm ($\epsilon = 9.9(1) \times 10^3$ M^{-1} cm^{-1}). IR (KBr pellet, cm^{-1}): 3500–3200, 3096, 1726, 1664, 1553, 1400, 1199, 1140, 856, 799, 765, 722. ^{1}H NMR (300 MHz, D_2O): 8.70 (d, 1 H, J = 5 Hz); 8.66 (d, 1H, J = 5 Hz); 8.26 (br s, 1H); 8.25 (br s, 1H); 7.78 (dd, 1H, J = 5 Hz, 1 Hz); 7.74 (dd, 1H, J = 5 Hz, 1 Hz); 4.51 (q, 1H, J = 7 Hz); 1.55 (d, 3H, J = 7 Hz). ^{13}C NMR (75 MHz, DMSO-d_6): 173.4 (COOH); 165.7, 164 (CONH); 155.5, 154.9, 150.2, 149.9, 142.1, 139.2, 123.1, 121.9, 119.0, 118.1 (bipy ring carbons); 48.2 (CH); 16.6 (CH_3).

Fe(Ala-bipy)$_3$. When iron(II) was added to a solution of Ala-bipy, a red color appeared, characteristic of formation of an Fe(bipy)$_3$ complex. The appearance of the complex was followed by UV–vis spectroscopy and by HPLC. Three equivalents of Ala-bipy were required for each iron cation. For Fe(Ala-bipy)$_3$: UV–vis (pH 4.8 acetate) λ_{max} = 310 nm ($\epsilon = 2.94(8) \times 10^4$ M^{-1} cm^{-1}), 540 nm ($\epsilon = 1.68(1) \times 10^4$ M^{-1} cm^{-1}). K_b was measured[10] as $2(1) \times 10^{16}$. CD of the crude iron complex showed that the molar ellipticity between 300 and 350 nm was $0(2) \times 10^4$ deg cm^{-2} dmol^{-1}, which corresponds to at most 2% diastereomeric excess for either meridional isomer (see Figure 3). Reverse-phase HPLC with acidic, neutral, or basic eluents at room temperature failed to resolve all four isomers and the free ligand. However, the components could be separated if the column was cooled. A 25-cm Vydac 300-Å-pore C_4 semiprep column was chilled to 0 °C in an ice bath. The flow rate was 3 mL/min (even at this reduced flow rate, the back-pressure was 4000 psi), the buffer 25 mM phosphoric acid/triethyl amine at pH 6.5 with 5% CH_3CN, detector set at 310 nm. Under these conditions, retentions times were 5.4 min for the Λ *fac*, 6.0 min for the Δ *fac*, 6.6 min for the Δ *mer*, and 6.9 min for the Λ *mer* isomer. The latter two isomers were incompletely resolved, but pure samples could be collected if the overlapping fractions were discarded. Free monomer eluted at 8.3 min. The ratio of the isomers was determined to be 12(2):12(2):76(2) for the Λ facial, the Δ facial, and the meridional isomers, respectively.

Circular dichroism samples were in the range $(2–9) \times 10^{-5}$ M metal complex, in pH 6.5 phosphate/TEA buffer containing 5% acetonitrile. Molar ellipticities of the metal-based CD bands at 222 and 319 nm, respectively, were calculated (in deg cm^{-2} dmol^{-1}). Δ *mer*: $+2.5(5) \times 10^4$, $-1.0(4) \times 10^6$. Λ *mer*: $-2.0(5) \times 10^4$, $+8(4) \times 10^5$. Δ *fac*: $+2.0(5) \times 10^4$, $-7(4) \times 10^5$. Λ *fac*: $-3.0(5) \times 10^4$, $+2(1) \times 10^6$.

4-(Ala-Glu-Gln-Leu-Leu-Gln-Glu-Ala-Glu-Gln-Leu-Leu-Gln-Glu-Leu-CONH$_2$)-4′-(COOH)-2,2′-bipyridine (Pepy). Pepy was synthesized and characterized as described previously.[7] Pepy has λ_{max} of 295 nm ($\epsilon = 1.17 \times 10^4$ M^{-1} cm^{-1}). The peptide is water-soluble at pH greater than 4. The CD spectrum is consistent with a mixture of helical and random coil structures; the helical content was estimated as 41% at pH 4.8 and 34% at pH 5.3. The molecular weight determined by sedimentation equilibrium centrifugation was 2.9×10^3 for a 1×10^{-3} M sample, 2.4×10^3 for a 5×10^{-4} M sample, and 2.3×10^3 for a 2.5×10^{-4} M sample at pH 4.8. When these values are extrapolated to zero concentration, the molecular weight is 2.1×10^3 (1.980×10^3 calculated). Electrospray MS: found 1981 (M + H), 2003 (M + Na).

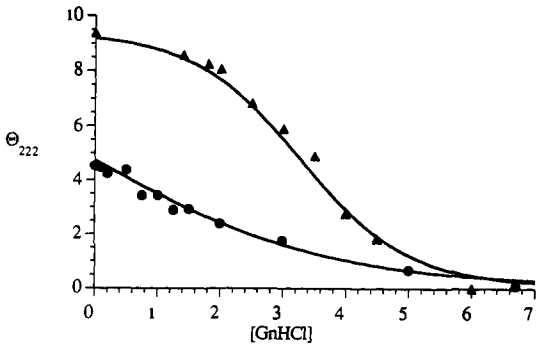

Figure 4. GnHCl denaturation of pepy (circles) and Fe(pepy)$_3$ (triangles). The concentration of pepy was 1.1×10^{-4} M in both experiments. The solid lines show the fits calculated from the two-state model.

The free energy of folding was determined using the two-state model.[4,14] CD samples contained 1×10^{-4} M peptide in 25 mM pH 4.8 acetate buffer along with varying concentrations of GnHCl. CD spectra were acquired in a 0.2-mm cell. The spectrum of this 15-mer did not show a plateau region at low concentrations of denaturant, although a plateau is present at high concentrations of denaturant (Figure 4). We assumed that the molar ellipticity of the "folded" state was the same for pepy as it is for Fe(pepy)$_3$, 28 800 deg mol^{-1} cm^{-2}, and that the molar ellipticity of the unfolded state was the plateau value, 1030 deg mol^{-1} cm^{-2}. Two experiments gave results that were identical within experimental error. Using these values, $\Delta G°_f$, the standard free energy of folding the protein from 3% to 86% helicity, is calculated as 0.00(2) kcal/mol; the protein is half-denatured at 0.00(6) M GnHCl, and m is 0.33(1) kcal mol^{-1} M^{-1}. These parameters were used to calculate the expected $[\theta]_{222}$ as a function of [GnHCl]; the fit to the experimental data is excellent, as shown in Figure 4.

ΔG_{eq}, the free energy of folding the protein from its unfolded value of 3% helicity to the observed equilibrium value of 41% helicity, was calculated within the two-state model using the standard free energy and the free energy of mixing,[15] as shown in eq 1. X_i represents the mole fraction of species i[16] and $\Delta G°_f$ is the standard free energy of folding. Using this method, ΔG_{eq} is calculated as –0.41 kcal/mol.

$$\Delta G_{eq} = X_f \Delta G°_f + \Delta G_{mix}; \quad \text{where } \Delta G_{mix} = X_f \ln X_f + X_u \ln X_u \tag{1}$$

Fe(pepy)$_3$. The iron complex of pepy formed when 1 equiv of freshly prepared $Fe(NH_4)_2(SO_4)_2 \cdot 6H_2O$ solution was added to 3 equiv of dissolved pepy. As the complex formed, a new UV–vis spectrum grew in, with isosbestic points at 270 nm ($\epsilon = 6.54 \times 10^3$ M^{-1} cm^{-1}) and at 294.5 nm ($\epsilon = 1.12 \times 10^4$ M^{-1} cm^{-1}). The spectrum of Fe(pepy)$_3$ has absorbance maxima at (λ_{max}, ϵ (M^{-1} cm^{-1})) 311 nm, 3.20×10^4; 380 nm, 1.1×10^4; and 545 nm, 1.47×10^4. The metalloprotein is soluble in water above pH 4, but in basic solution, it undergoes dissociation followed by irreversible oxidation of the iron(II) and formation of Fe_2O_3. The molecular weight, calculated as 5998, was determined by electrospray MS (found m/z 1999.3 [Fe(pepy)$_3$]$^{3+}$; 1499.8 [Fe(pepy)$_3$ + H]$^{4+}$) and by sedimentation equilibrium centrifugation in pH 4.8 buffer (found $5.9(7) \times 10^3$).

The free energy of folding was determined by denaturation with guanidine hydrochloride.[4] Samples contained a final concentration of 3.3×10^{-5} M Fe(pepy)$_3$ in 25 mM pH 4.8 acetate buffer with varying concentrations of GnHCl. CD spectra were acquired in a 0.2-mm cell. Fe(pepy)$_3$ showed plateau regions at low and high concentrations of denaturant and was assumed to be completely folded at 0 M GnHCl and completely denatured at 6.67 M GnHCl. The molar ellipticities of these states were 28 800 and 1030 deg mol^{-1} cm^{-2}, respectively. Two experiments gave results identical within experimental error. The free energy of folding Fe(pepy)$_3$ at 0 M GnHCl was calculated as –2.3(2)

(14) Peptide folding curves can also be analyzed with multiple-state models, but the two-state model seems to be an adequate approximation. For example, for a set of 10 short peptides, the ΔG_f calculated by the two-state and by a Zimm–Bragg analysis differed by less than 0.1 kcal/mol, see: (a) Lyu, P. C.; Liff, M. I.; Marky, L. A.; Kallenbach, N. R. *Science* **1990**, *250*, 669–673, Table 1. (b) Gans, P. J.; Lyu, P. C.; Manning, M. C.; Woody, R. W.; Kallenbach, N. R. *Biopolymers* **1991**, *31*, 1605–1614, Table II.

(15) Atkins, P. W. *Physical Chemistry*, 4th ed; Freeman: New York, 1990; Chapter 7.

(16) X_i is determined from the total helicity and the helicity of each species; in the case of pepy, it is 0.46 for the folded and 0.54 for the unfolded.

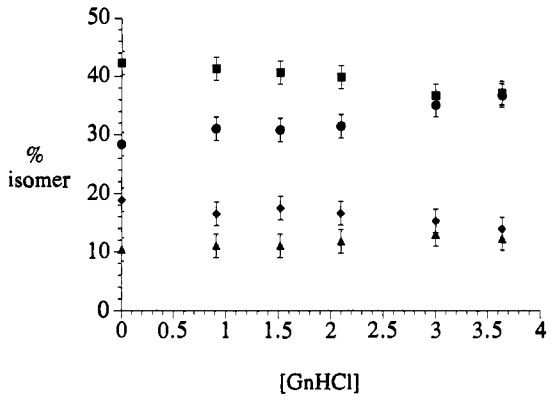

Figure 5. Isomer distribution in $Fe(pepy)_3$ made from denatured pepy. Pepy was incubated with the indicated concentration of guanidinium hydrochloride before addition of Fe(II).

kcal/mol; the protein is half-folded at a 3.3(1) M concentration of GnHCl and m was determined to be 0.70(5) kcal mol^{-1} M^{-1}.

The reverse-phase HPLC conditions for resolution of the isomers of $Fe(pepy)_3$ were as follows: 25-cm Microsorb 300-Å-pore C_4 analytical column at 1 mL/min or 25-cm Vydac 300-Å-pore C_4 semiprep column at 4 mL/min; 20-μL sample loop for the analytical column or 1-mL loop for the semiprep column; eluent A = 20% CH_3CN/80% water/0.1% TFA; eluent B = 80% CH_3CN/20% water/0.1% TFA; UV–vis detector set at 220, 294.5, or 545 nm; good separation is obtained with linear gradients of 35%–55%B to 85%B in 12–20 min. For example, with a semipreparative column and a gradient of 50%B to 88%B in 12 min, the retention times for pepy and the four isomers were as follows: pepy 6.74 min, Δ *mer* 10.38 min, Λ *mer* 11.19 min, Δ *fac* 12.48 min, Λ *fac* 14.45 min. UV–visible spectra of each of the isomers were obtained with a diode-array HPLC detector; the spectra were superimposable.

In order to quantitate the ratios of isomers in the absence and presence of guanidinium hydrochloride (GnHCl), samples with 3×10^{-4} M pepy and different concentrations of GnHCl in pH 4.8 buffer were mixed with a stoichiometric amount of freshly prepared $Fe(NH_4)_2(SO_4)_2 \cdot 6H_2O$. After a 20-min incubation period, the solutions were analyzed by HPLC. The isomer ratios were determined by cutting out and weighing peaks from the HPLC trace. The ratios at 0 M GnHCl were 29(2)%:43(2)%:17(2)%:12(2)% for the Δ *mer*, Λ *mer*, Δ *fac*, and Λ *fac* isomers, respectively. The ratios altered smoothly in the presence of increasing concentrations of GnHCl, as shown in Figure 5, until limiting values of 36(2)%:37(2)%:14(2)%:12(2)% were attained in 3.67 M GnHCl.

High-resolution NMR was used to study the arrangement of ligands around the metal. For each experiment, a purified isomer was dissolved in 0.5 mL of 10 mM pH 7 phosphate buffer in D_2O, DSS was added as a reference compound, and the solution was lyophilized several times from D_2O. Samples were about 0.2 mM in the metal complex. Samples were stored on ice to retard isomerization. NMR spectra were obtained on a 500-MHz Bruker spectrometer with probe temperature maintained at 287 K. Low decoupler power was applied to 22 points covering the HDO peak for 2.5 s to presaturate it, and then 100–200 FIDs were acquired. Spectra of the bipyridine regions of the isomers are shown in Figure 7. The aliphatic regions for all four isomers are very similar, with peaks at δ values of 0.85–0.95, Leu-C*H*$_3$; 1.43, d (J = 7 Hz), Ala-C*H*$_3$; 1.50–1.70, Ala-C*H*$_3$ and Leu β-C*H*$_2$ and δ-C*H*; 1.90–2.03, Glu/Gln β-C*H*$_2$; 2.25–2.40, Glu/Gln γ-C*H*$_2$; 4.20–4.32, α-C*H*. The peaks, with the exception of the Ala-C*H*$_3$ at 1.43 δ, were ill-resolved at temperatures between 14 and 33 °C. After a spectrum had been acquired, an aliquot of the sample was analyzed by HPLC to determine the sample purity. The results of this analysis were as follows. Δ *mer*: 88%, 8% pepy, 4% Λ *mer*. Λ *mer*: 94%, 4% pepy, 3% Δ *mer*. Δ *fac*: 84%, 10% pepy, 6% Λ *mer*. Λ *fac*: 97%, 2% Δ *mer*.

CD spectra for the four isomers are shown in Figure 8. For CD spectroscopy, a lyophilized isomer was taken up in 50 μL of ice-cold 10 mM pH 6.5 acetate buffer and then diluted with 250 μL of ice-cold 100 mM pH 5.2 acetate. The sample was centrifuged to check that all material was in solution. The pH was adjusted to between 5.2 and 5.4 with a few microliters of 0.5 M sodium acetate or acetic acid. Samples were kept frozen on dry ice until the measurement. Afterwards, an aliquot of the sample was analyzed by HPLC to determine the isomer distribution. The results of this analysis were as follows. Δ *mer*: 83% Δ *mer*, 8% Λ *mer*, 4% Λ *fac*, 4% pepy. Λ *mer*: 19% Δ *mer*, 81% Λ *mer*. Δ *fac*: 2% Δ *mer*, 6% Λ *mer*, 85% Δ *fac*, 3% Λ *fac*, 5% pepy. Λ *fac*: 10.5% Δ *mer*, 89.5% Λ *fac*. After correcting for the excess of Δ or Λ isomers, the calculated molar ellipticities at 319 nm for the Δ *mer*, Λ *mer*, Δ *fac*, and Λ *fac* isomers were −8.2(8), +7.0(5), −6.5(5), and +8.2(5) × 10^5 deg cm^{-2} $dmol^{-1}$, respectively. The helical content of the four isomers at pH 5.3 was estimated from the per-residue molar ellipticity as 51(3)% for the Δ *mer*, 92(3)% for the Λ *mer*, 52(3)% for the Δ *fac*, and 47(3)% for the Λ *fac* isomer. These values contain a correction for a metal-based band which is present in the model compound at 222 nm; the magnitude of the correction is in each case less than 9% helicity.

Kinetics. Initial rates of isomerization and dissociation of the isomers of $Fe(pepy)_3$ were determined by reverse-phase HPLC. In a typical experiment, a sample of a pure isomer of $Fe(pepy)_3$ was dissolved in 20 μL of 10 mM pH 6.5 acetate buffer. Ice-cold 100 mM pH 5.2 acetate buffer (150 μL) was added; the final concentration of isomer ranged between 2 and 5×10^{-5} M. The pH was adjusted to between 5.2 and 5.4 with 0.5 M acetic acid, and then the sample was divided into aliquots and frozen on dry ice. For each run, a 50-μL aliquot was thawed to room temperature. Portions of 5 μL were injected onto the HPLC column at 25–60-min intervals for 3–10 h. The accuracy of the integrator was checked by recording some spectra on strip chart paper, enlarging them, cutting out the peaks, and weighing them. The ratios obtained in this manner agreed with the ratios reported by the integrator.

For $Fe(pepy)_3$, the percentages of the four isomers and the free ligand were measured and normalized to sum to 100%. In all cases, they accounted for at least 85% of the intensity found by the integrator; the balance was base-line noise and buffer peaks. Initial rates were determined by a linear least-squares fit to a plot of % isomer vs time over the first 10%–20% of the reaction. Over this time period, the plots were linear. Rate constants were calculated by dividing the initial rates by the initial percentage of the reacting isomer, which was always >85%. Each isomer was run at least three times, and the rate constants were averaged.

The initial rates of interconversion of the four isomers of $Fe(Ala\text{-}bipy)_3$ were determined in a similar way. $Fe(Ala\text{-}bipy)_3$ was resolved, and the collected fractions were frozen on dry ice. The samples were not lyophilized but were thawed to room temperature and used as they were, in pH 6.5 phosphate/TEA buffer containing 5% acetonitrile. The isomerization of $Fe(Ala\text{-}bipy)_3$ was followed at 2–5 time points. The ratios of the four metal isomers were determined by cutting out and weighing peaks from the HPLC traces. The rate constant for dissociation of $Fe(Ala\text{-}bipy)_3$ in the mixture of isomers was measured spectroscopically following Basolo and co-workers' method.[17] It was $1.6(2) \times 10^{-4}$/min. The observed raw rates of isomerization were adjusted to account for the dissociation reaction, assuming that the isomers all lose Ala-bipy at the same rate.

For both metal complexes, the equilibrium constant between each pair of isomers was used to calculate reverse rates for every measured rate; the agreement of calculated and observed rates was usually within experimental error. The rate data were smoothed by averaging the calculated and observed rates; these smoothed data are reported in Table 1.

Results

Synthesis and Characterization of Pepy. 4,4′-Dicarboxylic acid-2,2′-bipyridine was covalently attached to the N terminus of an amphiphilic 15-residue peptide, as described earlier.[7,18] Sedimentation equilibrium centrifugation shows that the peptide self-aggregates slightly[19] at high concentrations but is monomeric at the concentrations used for CD, UV–vis, and GnHCl denaturation. The observed CD spectrum is consistant with a two-state helix–coil equilibrium, with a helix content of 41% at pH 4.8 and 34% at pH 5.3. The two-state model was used to analyze the GnHCl denaturation.[14] The standard free energy of folding, $\Delta G°_f$, was determined to be 0.00(2) kcal/mol; this is the energy required

(17) Basolo, F.; Hayes, J. C.; Neumann, H. M. *J. Am. Chem. Soc.* **1954**, *76*, 3807–3809.

(18) Lieberman, M.; Tabet, M.; Tahmassebi, D.; Zhang, J.; Sasaki, T. *Nanotechnology* **1991**, *2*, 203–205.

(19) The molecular weight determined by sedimentation equilibrium centrifugation for a 2.5×10^{-4} M sample was 2.3×10^3 g/mol (1.98×10^3 calculated). Clearly, some aggregation takes place; the aggregation state is unknown. We calculate that, if the peptide dimerizes, 71% of the peptide is present as monomer: MW_{avg} = [0.72(1980) + 0.14(3960)]/0.86 = 2303 g/mol. Higher aggregation states predict larger amounts of peptide present as the monomer.

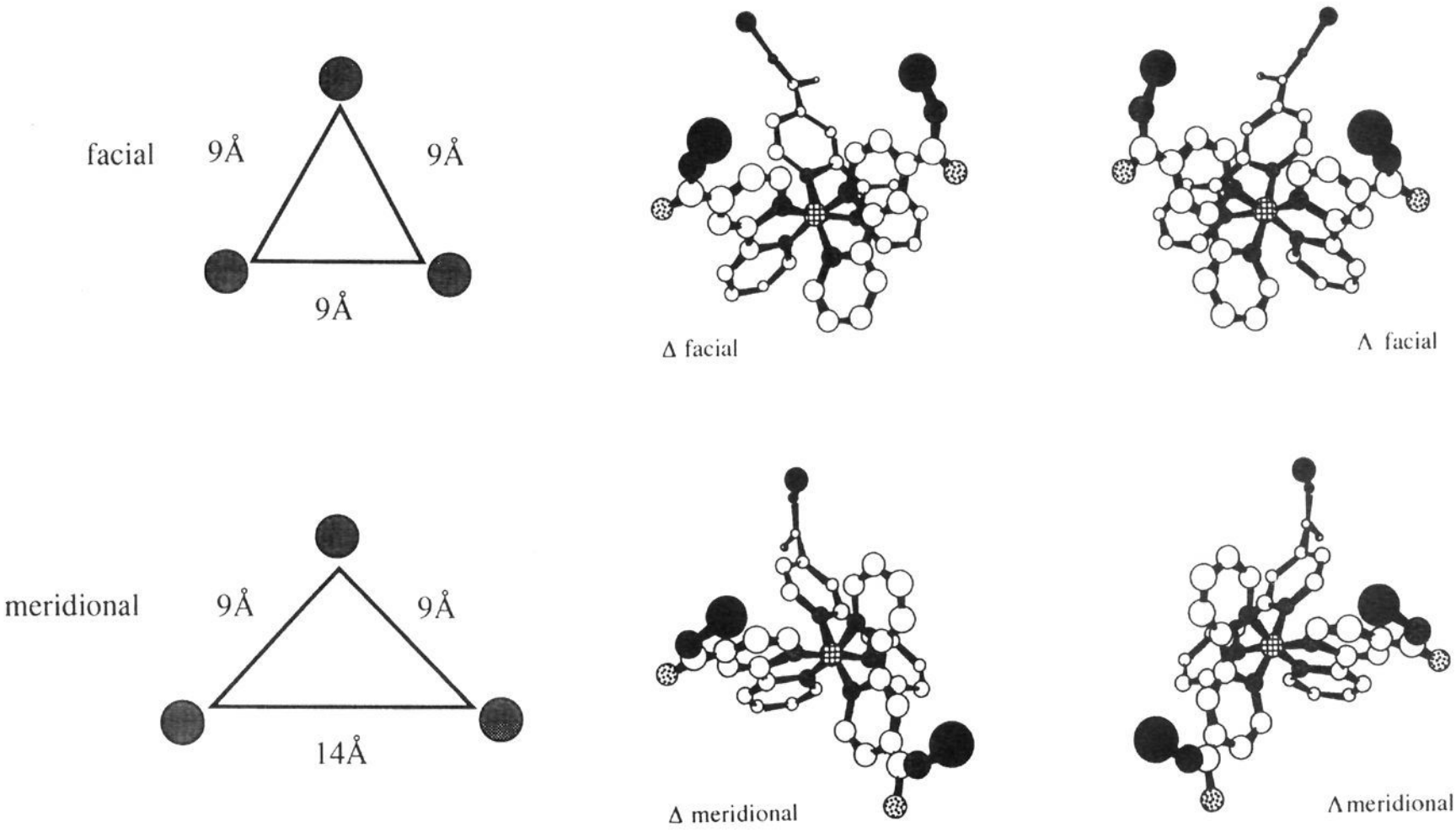

Figure 6. The four isomers of Fe(4-R-4′-carboxy-2,2′-bipyridine)$_3$, R = A-CONH$_2$ or AEQLLQEAEQLLQEL-CONH$_2$. The dark spheres represent C_α of alanine. The triangles show the geometrical disposition of the three R groups on facial and meridional templates.

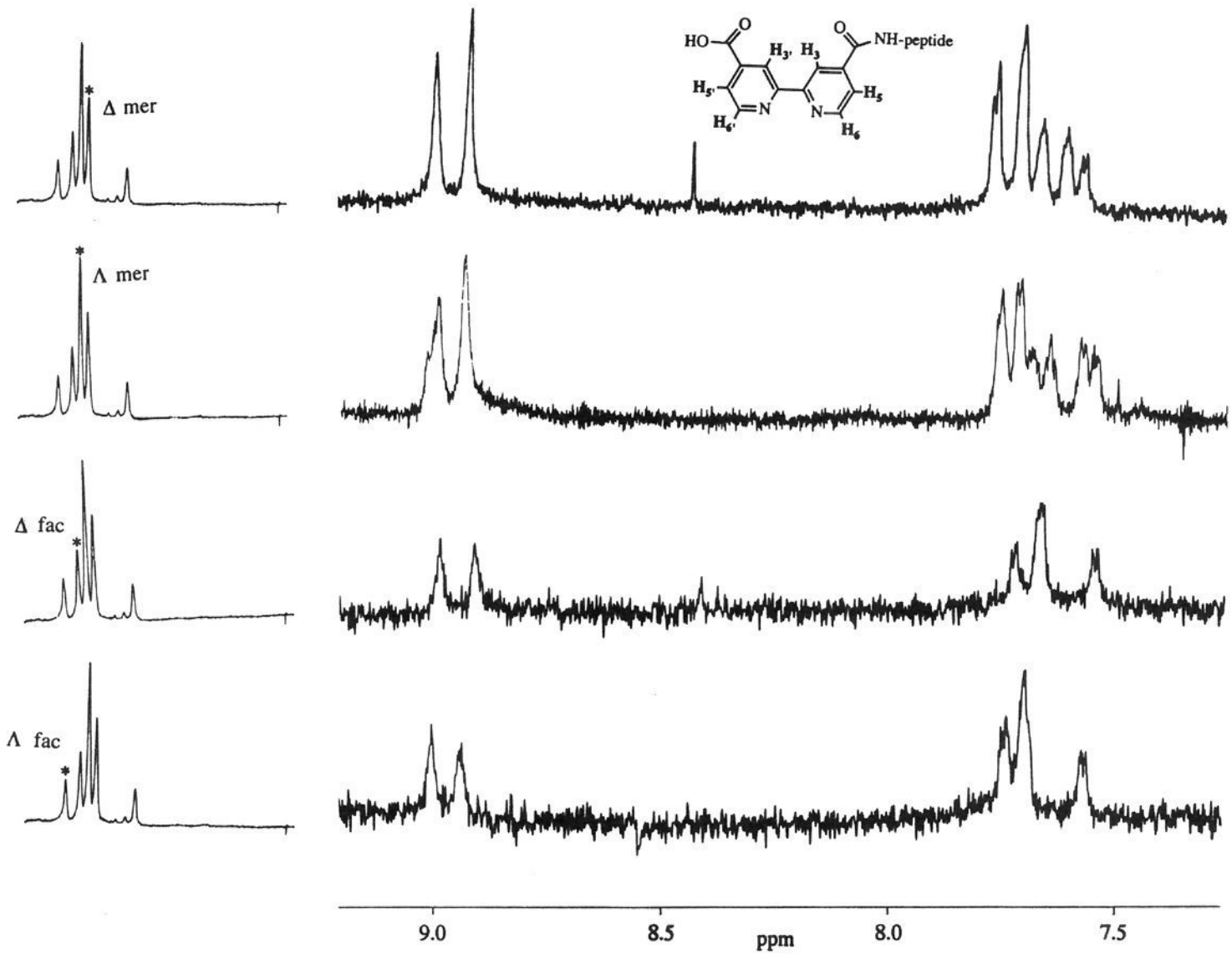

Figure 7. NMR spectra of the bipyridine region of pure isomers of Fe(pepy)$_3$. An asterisk on the accompanying HPLC trace identifies each isomer.

to go from the completely folded to the completely unfolded state. However, in water at pH 4.8 some of the peptide is folded and some is unfolded, and it is ΔG_{eq}, the free energy of attaining this equilibrium state, that we would like to ascertain. Within the two-state model, ΔG_{eq} depends on the free energy of folding a fraction of the peptides and the free energy of mixing the folded and unfolded molecules, as shown in eq 1, and is calculated as –0.41 kcal/mol.

Preparation and Characterization of Fe(pepy)$_3$. Pepy trimerizes in the presence of Fe(II). As the trimer's spectrum grows in, it shows several isosbestic points, which demonstrates that only two species—free pepy and Fe(pepy)$_3$—are present in significant

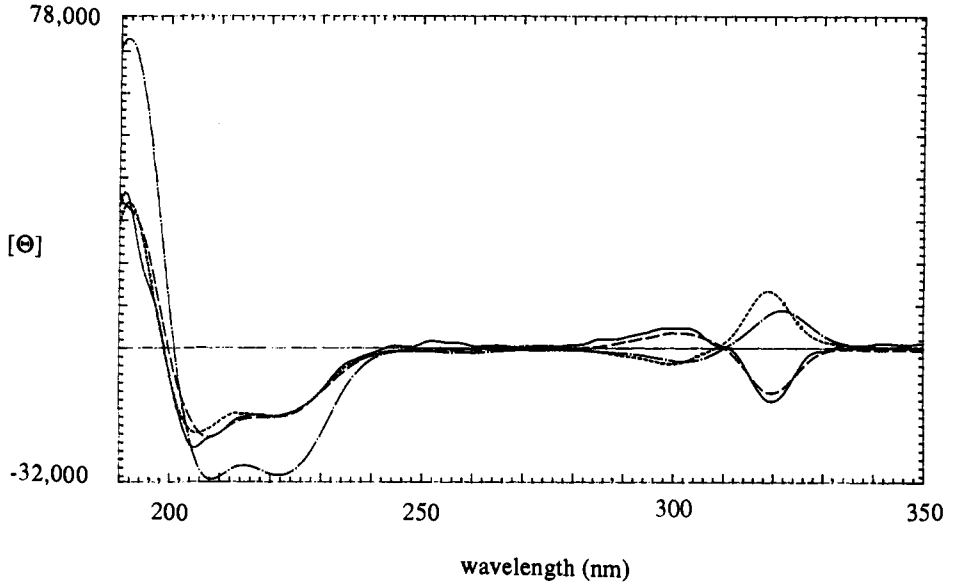

Figure 8. CD spectra of isomers of Fe(pepy)$_3$: Δ meridional (solid, 71% de); Λ meridional (dot–dash, 62% de); Δ facial (dashed, 78% de); Λ facial (dotted, 79% de). Units of [Θ] are deg cm^{-2} dmol^{-1}.

Table 1. Rates of Isomerization for Fe(Ala-bipy)$_3$ and Fe(pepy)$_3$

reactant	k_D (× 10^{-4} min^{-1})	$k_{\Delta fac}$ (× 10^{-4} min^{-1})	$k_{\Lambda fac}$ (× 10^{-4} min^{-1})	$k_{\Delta mer}$ (× 10^{-4} min^{-1})	$k_{\Lambda mer}$ (× 10^{-4} min^{-1})
Fe(Ala-bipy)$_3$ Δ*fac*	16(2)	−27(14)	0.7(7)	2.9(5)	17(5)
Fe(Ala-bipy)$_3$ Λ*fac*	16(2)	0.6(6)	−15(5)	11(3)	2(1)
Fe(Ala-bipy)$_3$ Δ*mer*	16(2)	0.8(2)	4(1)	−9.0(5)	5(1)
Fe(Ala-bipy)$_3$ Λ*mer*	16(2)	6(2)	1.2(4)	6(1)	−20(12)
Fe(pepy)$_3$ Δ*fac*	2.3(3)	−4.3(3)	0.19(4)	0.3(2)	1.0(2)
Fe(pepy)$_3$ Λ*fac*	4.8(3)	0.27(6)	−11.8(5)	3(2)	0.8(2)
Fe(pepy)$_3$ Δ*mer*	1.7(2)	0.16(9)	1.2(5)	−4.0(3)	2.1(6)
Fe(pepy)$_3$ Λ*mer*	2.3(4)	0.38(6)	0.22(6)	1.4(4)	−4.8(5)

amounts. On binding iron, the bipyridine transition shifts 16 nm to the red of that of pepy, and charge-transfer bands give rise to strong absorbances at 380 and 545 nm. The binding constant of 9(4) × 10^{16} was determined spectroscopically.[10] Electrospray mass spectrometry showed peaks at the m/z expected for [Fe(pepy)$_3$]$^{3+}$ and [Fe(pepy)$_3$]$^{4+}$, along with other peaks that were consistent with loss of one or two ligands, a reaction that probably occurs during ionization. Species with one or two peptides bound to the iron are never observed in solution by HPLC or UV–vis spectroscopy.[20] The molecular weight was measured as 5.9(7) × 10^3 g/mol by sedimentation equilibrium centrifugation, indicating that the metalloprotein neither dissociates nor self-associates in solution. CD spectroscopy was used to probe the secondary structure content of the protein. Upon trimerization, the helicity increases from 41% to 86% at pH 4.8 (34% to 73% at pH 5.3), and a new CD band appears at 319 nm with intensity about 10% of the 222-nm band. The secondary structure of the metalloprotein has a moderate thermodynamic stability, as determined by GnHCl denaturation; $\Delta G°_f$ is calculated as −2.3-(2) kcal/mol using a two-state model.

Octahedral complexes derived from three unsymmetrical bidentate ligands are expected to have four diastereomers.[21] There are two geometrical isomers, facial and meridional, each of which exists in two chiral forms (Figure 6). Indeed, careful analysis of Fe(pepy)$_3$ by reverse-phase HPLC shows that it consists of four species (Figure 7). These metalloprotein species are assigned as the four diastereomers around the iron tris(chelate) core. They show UV–visible spectra that are nearly superimposable with one another and with the original Fe(pepy)$_3$ mixture, and they slowly interconvert with one another. Collected over dry ice, lyophilized, and stored at −4 °C, the isomers are stable for months. When iron is added to a solution of pepy at pH 4.8, the four isomers form initially in a 29:43:17:12 ratio (in the order of elution). Allowing the solution to stand at room temperature for three days does not alter this ratio. When the pepy was treated with guanidinium hydrochloride before the addition of iron, the ratio changed smoothly, reaching values of 36:37:14:12 at 3.67 M denaturant (Figure 5). The ratio expected from a statistical distribution of isomers is 37.5:37.5:12.5:12.5 for the Δ and Λ meridional and Δ and Λ facial isomers, respectively. This statistical ratio is generally observed in simple unsymmetric tris(chelate) complexes.[22] The ratio of isomers of Fe(pepy)$_3$ formed from pepy under denaturing conditions suggests that the two species that elute first are meridional and the two that elute last are facial. The change in isomer ratio shown in Figure 5 indicates that some interaction between the peptides skews the relative stabilities of the isomers.

The assignments of the C_3-symmetric facial isomers and the C_1-symmetric meridional isomers were confirmed by ^{1}H NMR spectroscopy (Figure 7). The protons corresponding to H5 or H5′[23] appear in the region between 7.5 and 7.7 δ, either as a doublet with J = 7 Hz (the value for the coupling constant between the H5 and H6 protons in pepy is 6 Hz) or as a more complicated multiplet. The doublet is consistent with C_3 symmetry, in which all of the bipyridine rings are equivalent, but the multiplet is only consistent with C_1 symmetry. On the basis of these spectra and of the effect of GnHCl on the isomer ratio, the first two peaks to elute were assigned as meridional isomers, and the last two

(20) The third binding constant of 2,2′-bipyridine for iron is 5 orders of magnitude higher than the first or second binding constants, so if dissociation occurs in solution, the complex is expected to fall completely apart.

(21) Cotton, F. A.; Wilkinson, G. *Advanced Inorganic Chemistry*; Wiley and Sons: New York, 1988.

(22) Cook, M. J.; Lewis, A. P.; McAuliffe, G. S. G.; Thomson, A. J. *Inorg. Chim. Acta* **1982**, *64*, L25–L28.

(23) (a) Ohsawa, Y.; DeArmond, M. K.; Hanck, K. W.; Moreland, C. G. *J. Am. Chem. Soc.* **1985**, *107*, 5383–5386. (b) Cook, M. J.; L., A. P.; McAuliffe, G. S. G.; Thomson, A. J. *Inorg. Chim. Acta* **1982**, *64*, L25–L28.

were assigned as facial isomers. The Δ or Λ configurations of $Fe(pepy)_3$ and $Fe(Ala\text{-}bipy)_3$ were assigned from the sign of the CD features between 300 and 330 nm, using the assignments of Milder et al.[24] for $\Delta(+)\text{-}[Fe(bpy)_3(ClO_4)]$. At pH 5.3, the Δ facial, Λ facial, and Δ meridional isomers have moderate helical content (52(3)%, 47(3)%, and 51(3)%, respectively). In contrast, the Λ meridional isomer is very helical (92(3)%). The helicity of the mixture calculated from the isomer ratio and helicities of the isomers is 68%, which agrees with the observed helicity of 73% at pH 5.3.

Synthesis and Characterization of Ala-bipy and its Fe(II) Complex, $Fe(Ala\text{-}bipy)_3$. 4-Alaninamido-4′-carboxy-2,2′-bipyridine, Ala-bipy, was synthesized by coupling alanine amide with the diacyl chloride of 4,4′-dicarboxy-2,2′-bipyridine (Scheme 1). Its UV–vis features were similar to those of pepy.

Ala-bipy formed a red iron complex with the expected stoichiometry of 1 Fe:3 Ala-bipy. Its binding constant was spectroscopically determined to be $2(1) \times 10^{16}$. Four isomers of $Fe(Ala\text{-}bipy)_3$ were observed by reverse-phase HPLC at 0 °C (Figure 3), although the last two isomers were poorly resolved. The ratio of the isomers determined by integration was 12:12:(76). Since there is no possibility of interaction between the alanine groups on the bipyridine ligands to cause a deviation from the statistical isomer ratio of 1:1:3:3, the first two peaks to elute were identified as the Δ and Λ facial and the later ones as the Λ and Δ meridional. The Δ and Λ enantiomers were assigned from the sign of the CD features between 300 and 330 nm, using the assignments of Milder et al.[24] for $\Delta(+)\text{-}[Fe(bpy)_3]ClO_4$. The CD spectrum of the equilibrium mixture of isomers was flat; since enantiomers are expected to have CD spectra that are equal in magnitude but opposite in sign, the maximum possible diastereomeric excess of either meridional isomer in the equilibrium mixture was 2%.

In addition to the features at 300–330 nm which were used to assign chirality, $Fe(Ala\text{-}bipy)_3$ has a CD feature at 222 nm, positive for the Δ isomers and negative for the Λ isomers. Since the "peptide" in the model compound is only one residue long, this band must be a metal-based feature. Presumably it is also present in the spectra of $Fe(pepy)_3$, masked by the intense 222-nm band that arises from α-helical structure. The reported helicities in the isomers of $Fe(pepy)_3$ have been corrected for the presence of this band, assuming that its molar ellipticity is the same in $Fe(pepy)_3$ as in $Fe(Ala\text{-}bipy)_3$. The magnitude of this correction corresponded to no more than 9% change in the apparent helicity for any of the isomers of $Fe(pepy)_3$.

Kinetics. When a solution of one of the isomers is allowed to stand, free pepy and the other three isomers slowly appear, as shown in Figure 9 for the Λ *fac* isomer of $Fe(pepy)_3$. There are 12 rate constants for interconversions of the four isomers. Equilibrium constants for the interconversions between each pair of isomers can be determined independently and accurately by integration of the peak intensities at equilibrium; each equilibrium constant is equal to the ratio of the forward and reverse rate constants for the interconversion of those two isomers. Other workers have studied similar inorganic isomerizations[25] by measuring k_f and K_{eq} for an interconversion and calculating k_r. We measured k_f, k_f, and K_{eq} and then used the more accurate K_{eq} values to smooth the data. A value of k_r was calculated from each k_f and K_{eq} and averaged with the observed k_r. The rate constants for ligand dissociation and the smoothed rate constants for interconversion of all four isomers of $Fe(pepy)_3$ and $Fe(Ala\text{-}bipy)_3$ are listed in Table 1. $Fe(pepy)_3$ isomerizes 5–20 times more slowly than does $Fe(Ala\text{-}bipy)_3$, depending on which interconversion is examined.

(24) Milder, S. J.; Gold, J. S.; Kliger, D. S. *J. Am. Chem. Soc.* **1986**, *108*, 8295–8296.

(25) (a) Gordon, J. G., II; Holme, R. H. *J. Am. Chem. Soc.* **1970**, *92*, 5319–5332. (b) Girgis, A. Y.; Fay, R. C. *J. Am. Chem. Soc.* **1970**, *92*, 7061–7072.

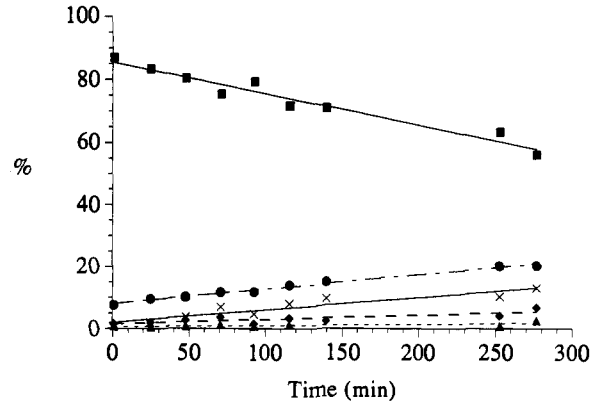

Figure 9. Isomerization of Λ *fac* isomer (squares) to form Δ *mer* (circles), Λ *mer* (diamonds), Δ *fac* (triangles), and free pepy (crosses). Components were resolved by reverse-phase HPLC and detected at 294.5 nm, which is an isosbestic point for pepy and $Fe(pepy)_3$.

Scheme 2. Calculation of ΔG_i from Formation Constants for $Fe(pepy)_3$ and $Fe(Ala\text{-}bipy)_3$

	free energy
(1) $Fe(II) + 3Ala\text{-}bipy \rightarrow Fe(Ala\text{-}bipy)_3$	$-RT\ln(K_{b,Ala\text{-}bipy})$
(2) $Fe(Ala\text{-}bipy)_3 + 3pepy_{41\%} \rightarrow Fe(pepy_{41\%})_3 + 3Ala\text{-}bipy$	$\Delta G_{ex} = 0$
(3) $Fe(pepy_{41\%})_3 \rightarrow Fe(pepy_{86\%})_3$	ΔG_i
(4) $Fe(II) + 3pepy_{41\%} \rightarrow Fe(pepy_{86\%})_3$	$-RT\ln(K_{b,pepy})$

$$\Delta G_i = -RT\ln(K_{b,pepy}/K_{b,Ala\text{-}bipy})$$

Scheme 3. Calculation of ΔG_i from Denaturation Energies of Pepy and $Fe(pepy)_3$

	free energy
(1) $Fe(pepy_{86\%})_3 \rightarrow Fe(pepy_{41\%})_3$	$-\Delta G_i$
(2) $Fe(pepy_{41\%})_3 + 3Ala\text{-}bipy \rightarrow Fe(Ala\text{-}bipy)_3 + 3pepy_{41\%}$	$\Delta G_{ex} = 0$
(3) $3pepy_{41\%} \rightarrow 3pepy_{3\%}$	$-3\Delta G_{eq} = 1.23$ kcal/mol
(4) $Fe(Ala\text{-}bipy)_3 + 3pepy_{3\%} \rightarrow Fe(pepy_{3\%})_3 + 3Ala\text{-}bipy$	$\Delta G_{ex} = 0$
(5) $Fe(pepy_{86\%})_3 \rightarrow Fe(pepy_{3\%})_3$	$\Delta G°_u = 2.3$ kcal/mol

$$\Delta G_i = -3\Delta G_{eq} + \Delta G°_u$$

Energies of Metastable States. Eventually, a constant isomer ratio forms. This equilibrium ratio is the same no matter which isomer we start with, and it is, within experimental error, identical to the ratio observed when iron and pepy are mixed.[26] The relative energy for each isomer, $\Delta\Delta G_{iso}$, is shown in eq 2.

$$\Delta\Delta G_{iso} = -RT\ln(X_{i,exp}/X_{i,stat}) \quad (2)$$

where $X_{i,exp}$ is the experimentally determined mole fraction of isomer i and $X_{i,stat}$ is the statistically predicted mole fraction. Relative energies for the Δ *fac*, Λ *fac*, Δ *mer*, and Λ *mer* isomers, respectively, with standard deviations in parentheses, are –0.18(2), +0.024(4), +0.16(1), and –0.080(4) kcal/mol.

Discussion

Mapping the Potential Well of $(Pepy)_3$. When $Fe(pepy)_3$ forms from monomeric pepy and iron, the measured binding energy includes terms from iron–ligand association and terms from peptide–peptide interactions. One can draw two independent thermochemical cycles to disentangle these effects (Schemes 2 and 3).

In the formation of the trimeric bundle, the peptides bind to iron, fold from their monomeric helical content of 41% to their full helical content of 86%, and pack into a bundle. We wish to determine the energy entailed in the last two steps, where the helices are interacting with one another. As shown in Scheme 2, the energy of interaction of the three helices, ΔG_i, may be

(26) The equivalence of the thermodynamic and kinetic isomer ratio suggests that the peptides undergo a preassociation before binding iron.

calculated from the ratio of formation constants for $Fe(pepy)_3$ and $Fe(Ala\text{-}bipy)_3$. We assume that the free energy of swapping an alanine residue for a peptide chain is 0. Ala-bipy mimics the electronic structure of pepy, and it has similar steric properties adjacent to the metal, so the formation constant for $Fe(Ala\text{-}bipy)_3$ ($K_{b,Ala\text{-}bipy} = 2(1) \times 10^{16}$) should be a good model for the metal–ligand bond strength and the loss of entropy entailed in orienting the three bipyridine ligands in space. The formation constant of $Fe(pepy)_3$ is 4.5 times larger than that of $Fe(Ala\text{-}bipy)_3$, which corresponds to a –0.9(7) kcal/mol energy of interaction at 298 °K.

ΔG_i may be independently estimated from measurements made on $Fe(pepy)_3$, as shown in Scheme 3. In this thermodynamic cycle, we first imagine that the peptides in $Fe(pepy)_3$ unfold in two steps and then compare this to a GnHCl denaturation. The peptides first unbundle and uncoil until they resemble monomeric pepy; this requires $-\Delta G_i$ kcal/mol. The noninteracting peptides are now swapped for Ala-bipy molecules, a step which we assume is thermoneutral, and the isolated peptides are completely unfolded at an energetic cost of $-3\Delta G_{eq}$ kcal/mol. The unfolded peptides are swapped back (again, we assume the swap is thermoneutral) to form $Fe(pepy)_3$ in which the peptide is completely denatured. The net effect is the same as denaturing $Fe(pepy)_3$ completely, for which reaction $\Delta G°_u$ was measured as +2.3(2) kcal/mol. From this thermodynamic cycle, ΔG_i is calculated to be –1.1(2) kcal/mol.

The potential energy well now begins to take shape; the peptides in $Fe(pepy)_3$ may be "unbundled" to a noninteracting state at a cost of about 1 kcal/mol, although to unfold them completely requires 2.3 kcal/mol.

Four Kinetically Trapped Protein States. Inorganic complexes of three unsymmetrical bidentate ligands have four diastereomeric forms (Figure 6), which act as different templates. The facial isomers position the bases of the helices at the vertices of an equilateral triangle with sides of length 9 Å. The meridional isomers position the bases of the helices at the vertices of an isosceles triangle with sides of length 9, 9, and 14 Å. The helices are only four turns long, about 20 Å, so a 5-Å difference in location of their origins is substantial. The facial and meridional isomers cannot possibly have the same tertiary structure.

Both facial and meridional isomers exist as pairs of propeller isomers. Diastereomeric interactions are present even in $Fe(Ala\text{-}bipy)_3$, which has an L amino acid near the chelating site; however, the known thermodynamic isomer ratio and CD spectrum of this complex show that neither the Δ or the Λ isomer predominates in the model compound. Bundles of right-handed helices are predicted to have a left-handed supercoiling interaction,[27] which ought to favor the Λ isomer of $Fe(pepy)_3$. Indeed, the Λ isomer is present in 5%–10% diastereomeric excess in the equilibrium mixture, and the Λ *mer* isomer is more helical than the Δ *mer*. However, this could be coincidence. Of the two facial isomers, the Δ is formed in 26% de, yet it is no more helical than the Λ isomer.[28]

The isomers of $Fe(Ala\text{-}bipy)_3$ form in the statistical ratio of 3:3:1:1, but the isomers of $Fe(pepy)_3$ deviate significantly from the statistical ratio. From the kinetic runs we know that the equilibrium ratio of $Fe(pepy)_3$ isomers at T_∞ is the same regardless of which isomer was present initially and is the same as the ratio which forms when iron and pepy are mixed. For $Fe(pepy)_3$, the thermodynamic and kinetic isomer distributions are identical. The relative energies for the Δ *mer*, Λ *mer*, Δ *fac*, and Λ *fac* isomers are +0.16(1), –0.080(4), –0.18(2), and +0.024(4) kcal/mol, respectively (see eq 2); a varience of less than 0.3 kcal/mol across four points in a fairly large piece of protein conformational space. $Fe(pepy)_3$ is not a well-folded protein, but a selection of molten globule states.

Barriers to Motion on the Potential Energy Surface of $(Pepy)_3$. In $Fe(pepy)_3$, interpeptide interactions are weak compared to metal–ligand interactions. When the metal complex isomerizes from one diastereomer to another, the peptides are dragged along willy-nilly. There are several possible mechanisms for the isomerization of metal complexes of unsymmetrical bidentate ligands, which may be distinguished by comparing the rates of different isomerizations.[29] For example, if isomerization proceds by the complete loss of a bipyridine ligand, the resulting four-coordinate iron species is expected to be high-spin and conformationally labile, as it presumably is during the stepwise formation of the tris complex from iron and ligand. A labile intermediate should result in promiscuous interconversion among all possible isomers, and because this is not observed, we can rule out an ML_2 intermediate. Likewise, it is possible to rule out a trigonal twist mechanism as the sole isomerization pathway, as this predicts large rates for the Δ–Λ isomerizations and a rate of 0 for everything else.

In fact, the Δ *mer* isomer of $Fe(pepy)_3$ produces Λ *mer* at twice the rate it produces Λ *fac*, which is in turn a great deal faster than the rate it produces the Δ *fac* isomer. Both of the meridional isomers of $Fe(Ala\text{-}bipy)_3$ and $Fe(pepy)_3$ prefer either inversion of chirality or double inversion over geometrical isomerization with retention of chirality. In contrast, the facial isomers show a preference for the double inversion, while inversion of chirality is very slow. The patterns of reactivity observed for both $Fe(Ala\text{-}bipy)_3$ and $Fe(pepy)_3$ are very similar and resemble those observed in other inert d^6 metal complexes, where both rhombic twist and dangling-ligand pathways have been proposed as the mechanism of isomerization.[30]

$Fe(pepy)_3$ isomerizes 5–20 times more slowly than $Fe(Ala\text{-}bipy)_3$. The heights of activation barriers to isomerization in the metalloprotein species have contributions both from the inorganic core and from ligand–ligand interactions in the transition state. The contribution of the inorganic core should be the same in $Fe(pepy)_3$ as they are in $Fe(Ala\text{-}bipy)_3$; however, if the peptides must rearrange during an isomerization, the energy of the transition state will be increased by an amount equal to the barrier to that rearrangement on the three-helix bundle potential energy surface. The energies of the barriers on the protein potential energy surface, *where the metal's contribution has been excluded*, were calculated from the ratios of rate constants for isomerization of $Fe(Ala\text{-}bipy)_3$ and $Fe(pepy)_3$ as shown in eq 3.

$$\Delta\Delta G^{\ddagger} = -RT \ln(k_{pepy}/k_{Ala\text{-}bipy}) \qquad (3)$$

where k_{pepy} and $k_{Ala\text{-}bipy}$ are the rate constants for a particular isomerization in $Fe(pepy)_3$ and $Fe(Ala\text{-}bipy)_3$ and $\Delta\Delta G^{\ddagger}$ is the height of the barrier to the corresponding rearrangement of the three peptides. Note that these value are really upper limits to the activation energies; there is no guarantee that the pathway for rearrangement used by the metal complex will correspond to the lowest barriers available on the protein's potential energy surface.

Figure 10a is a schematic three-dimensional representation of the potential energy surface for this parallel three-helix bundle protein. The potential energy wells that correspond to the two Δ isomers are on the right-hand side of the figure, the two Λ isomers are on the left, the facial isomers are at the back of the figure, and the meridional isomers at the front. The relative energies of these four wells were calculated from the experi-

(27) Cohen, C.; Parry, D. A. D. *Proteins: Struct., Funct., Genet.* **1990**, *7*, 1–15.

(28) Since $Fe(pepy)_3$ consists of about 3 times as many *mer* isomers as *fac* isomers and the molar ellipticities are similar, the Λ configuration predominates in the CD signal of the equilibrium mixture.

(29) (a) Serpone, N.; Bickley, D. G. *Prog. Inorg. Chem.* **1972**, *17*, 391–566. (b) Gordon, J. G., II; Holme, R. H. *J. Am. Chem. Soc.* **1970**, *92*, 5319–5332.

(30) (a) Gordon, J. G., II; Holme, R. H. *J. Am. Chem. Soc.* **1970**, *92*, 5319–5332. (b) Girgis, A. Y.; Fay, R. C. *J. Am. Chem. Soc.* **1970**, *92*, 7061–7072.

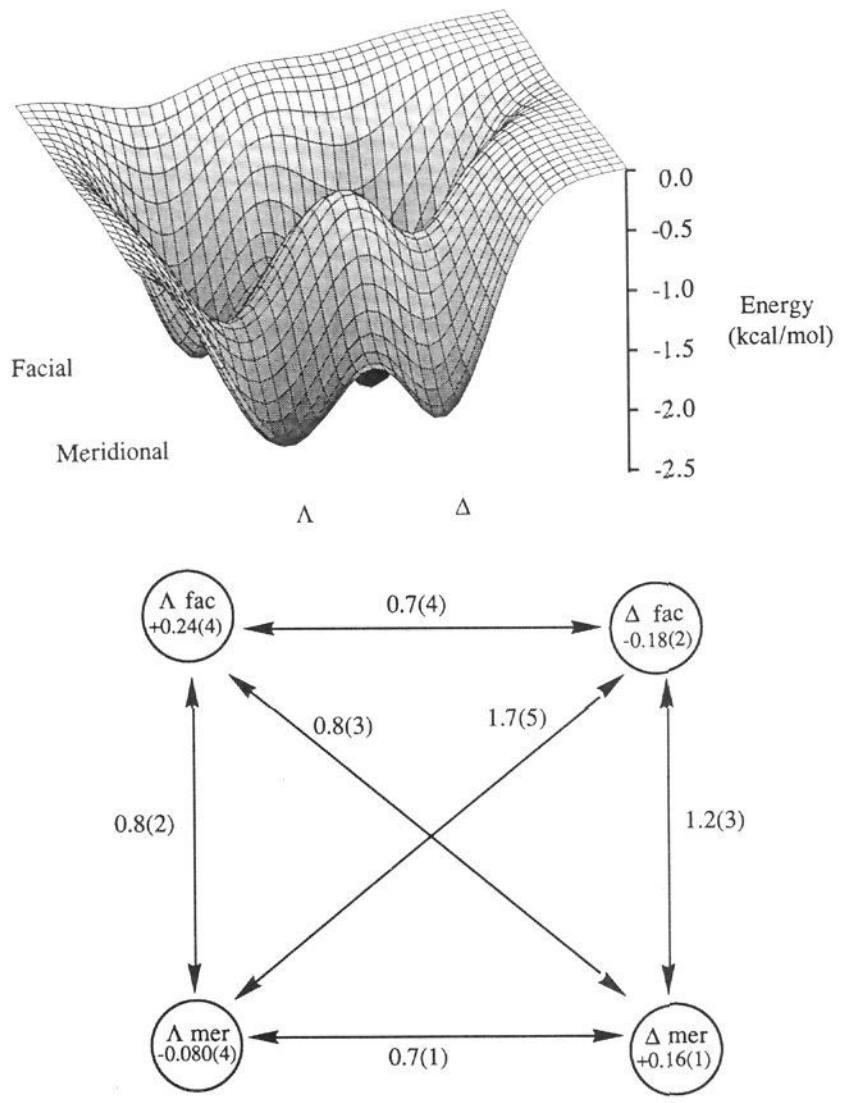

Figure 10. (a) Potential energy surface of a parallel three-helix bundle protein, $(pepy)_3$. The zero in energy corresponds to the completely denatured state. The four wells correspond to the metastable structures which form on the four metal templates. The energies of the metastable structures are all about –2.3 kcal/mol. Saddle points between different metastable protein structures were determined from kinetic measurements, as discussed in the text. (b) Heights of barriers on the potential energy surface of a parallel three-helix bundle that correspond to the indicated isomerizations of the inorganic core. The relative energies of the four metalloprotein species are indicated inside the circles. (kcal/mol, standard errors in parentheses.)

mentally determined perturbation of the isomer ratio in $Fe(pepy)_3$. The population-weighted average of the energies of the four isomers is –2.3 kcal/mol, the denaturation energy for the mixed isomers. The heights of activation barriers to the six transitions between pairs of isomers provide additional information about the potential energy surface; Figure 10b lists the experimentally determined maximal values for these barriers. Standard errors are shown in parentheses.[31]

The Δ–Λ isomerizations have relatively low barriers, ranging between 0.5 and 0.9 kcal/mol, with an average value of 0.7(3) kcal/mol. Interconversions of facial and meridional isomers of the same chirality have barriers ranging from 0.5 to 1.4 kcal/mol, with an average value of 1.0(3) kcal/mol. Double inversion, in which both geometrical and Δ–Λ isomerization occurs, has a barrier averaging 1.7(5) kcal/mol for the Δ *fac*–Λ *mer* isomerization, while the Λ *fac*–Δ *mer* isomerization averages 0.8(3) kcal/mol.

Molten globules have been assumed to pass from one state to another while retaining much of their secondary structure and compactness.[3] Although no mechanistic pathways for such conformational isomerizations have been demonstrated experimentally, molecular dynamics simulations of heteropolymers and proteins[32] show that transitions among compact states need not require significant unfolding. For the observable states in this molten globule-like protein, the barriers to isomerization are all smaller than the $\Delta G°$ for unfolding $Fe(pepy)_3$. Since the barrier to unfold the metalloprotein must be larger than $\Delta G°_u$, this rules out transition states where the protein is completely unfolded; thus, we have experimental evidence that the mechanistic pathways for transitions among all the substates in this molten globule-like protein avoid the unfolded state.[33] Likewise, for four out of the six interconversions, the three helices never completely "unbundle".

Structural Issues in Designed Proteins. We can say very little about the details of the interchain interactions in $Fe(pepy)_3$. Although the presence of metastable states allows us to study the energies of protein states in great detail, it gives little insight into the structure of the protein. The peptide portions of the Δ and Λ facial and Δ meridional isomers all have moderate helical content; a two-helix bundle with a third peptide uncoiled but associated with it in some way would be consistent with the observed helicity, as would a bundle of three partially helical peptides. The Λ meridional isomer, however, shows such high helicity that it is difficult to imagine any structure for it other than a three-helix bundle. Even so, its actual structure is probably significantly different from the intended structure. The hydrophobic surface of pepy's designed amphiphilic helix is composed of five leucine residues and two alanine residues. Rose and coworkers[34] analyzed crystal structures of 67 proteins and found that similar areas of hydrophobic surface can be buried in leucine–leucine and leucine–alanine interactions, more than can be buried in an alanine–alanine interaction. Leucine and alanine residues are expected to pack together without much specificity. For example, there are no interactions that would stop one helix from sliding up or down with respect to the other two. A CPK model of the Λ-meridional isomer suggests that, when the hydrophobic surfaces of all three helices associate, one helix must move up out of register with the other two by 2–3 Å. Thus, the contacts between helices within the hydrophobic core might be very different from those which we expected.

The structural characterization of *de novo* designed proteins has, by necessity, been quite indirect. There are only a handful of crystal structures[35] for designed proteins and no NMR solution structures. Since direct evidence for tertiary structure is the

(31) The barrier heights and errors are relatively insensitive to the smoothing procedure described in the Experimental Section. Using unsmoothed data does not alter any of the barriers by more than 0.2 kcal/mol, except the Δ–Λ facial isomerization barrier, which drops to 0 kcal/mol.

(32) (a) Shakhonovich, E.; Farztdinov, G.; Gutin, A. M.; Karplus, M. *Phys. Rev. Lett.* **1991**, *67*, 1665–1668, 3-D heteropolymer. (b) Camacho, C. J.; Thirumalai, D. *Proc. Natl. Acad. Sci. U.S.A.* **1993**, *90*, 6369–6372, 2-D heteropolymer. (c) Daggett, V.; Levitt, M. *Proc. Natl. Acad. Sci. U.S.A.* **1992**, *89*, 5142–5146, simulation of bovine pancreatic trypsin inhibitor. (d) Chan, H. S.; Dill, K. A. *J. Chem. Phys.* **1991**, *95*, 3775–3787, 2-D heteropolymer. (e) Miller, R.; Danko, C. A.; Fasolka, M. J.; Balazs, A. C.; Chan, H. S.; Dill, K. A. *J. Chem. Phys.* **1992**, *96*, 768–780, 2-D heteropolymers.

(33) In contrast to these easy transitions within a molten globule manifold of states, the transition from molten globule to folded protein may have a relatively high barrier. Baker et al.[5b] isolated a stable folding intermediate of α-lytic lysozyme with molten globule-like characteristics and estimated that the barrier between it and the folded state was >27 kcal/mol (the protein is normally biosynthesized with a promoter region that serves to lower this kinetic barrier and enable the protein to fold).

(34) Behe, M. J.; Lattman, E. E.; Rose, G. D. *Proc. Natl. Acad. Sci. U.S.A.* **1991**, *88*, 4195–4199.

(35) (a) Schafmeister, C. E.; Miercke, L. J. W.; Stroud, R. M. *Science* **1993**, *262*, 734. (b) Lovejoy, B.; Choe, S.; Cascio, D.; McRorie, D. K.; DeGrado, W. F.; Eisenberg, D. *Science* **1993**, *259*, 1288–1293. (c) Eisenberg, D.; Wilcox, W.; Eshita, S. M.; Pryciak, P. M.; Ho, S. P. *Proteins: Struct., Funct., Genet.* **1986**, *1*, 16–22. (d) Osterhout et al. used CD and NMR to determine secondary structure in a four-helix bundle protein, but did not observe any intrahelix NOEs: Osterhout, J. J., Jr.; Handel, T.; Na, G.; Toumadje, A.; Long, R. C.; Connolly, P. J.; Hoch, J. C.; Johnson, W. C., Jr.; Live, D.; Degrado, W. F. *J. Am. Chem. Soc.* **1992**, *114*, 331–337. (e) Mutter et al. report NMR cross peaks in a four-helix bundle protein between a unique phenylalanine residue on one helix and leucines on at least one other helix, but owing to the monotony of the sequence, could not assign sequence-specific resonances: Mutter, M.; Tuchscherer, G. G.; Miller, C.; Altmann, K.-H.; Carey, R. I.; Wyss, D. F.; Labhardt, A. M.; Rivier, J. E. *J. Am. Chem. Soc.* **1992**, *114*, 1463–1470. (f) Harbury, P. B.; Zhang, T.; Kim, P. S.; Alber, T. *Science* **1993**, *262*, 1401–1407. X-ray crystal structure of a parallel four-helix bundle.

exception rather than the rule, inferences about tertiary structure are often made on the basis of observations of secondary structure. For example, helical artifical proteins are made both by attaching helical segments to flexible templates (TASP approach) and by designing linear peptides with helical segments separated by turn sequences. The helical segments are expected to associate in defined ways, as for example by formation and aggregation of amphipathic helices, with consequent increases in secondary structure content. Observation of these predicted changes in secondary structure content has been cited as proof that the molecule has folded as designed.[36] In the case of $Fe(pepy)_3$, isolation of four metastable proteins shows that our earlier structural conclusion,[7] that the peptide prefers a C_3-symmetric facial template, is wrong. However, for proteins that are conformationally mobile, it may be impossible to detect multiple protein states.[37] As a gedanken experiment, imagine the substitution of a labile metal such as Co(II) for the inert Fe(II) in $Fe(pepy)_3$. The resulting metal complex would be able to isomerize quickly, as would a flexible organic template. The metalloprotein would show an average CD spectrum displaying a large increase in helical content. One might be tempted to decide that the molecule had folded as planned, when in fact at least four isoenergetic structures would be present, none necessarily possessing the designed C_3-symmetrical three-helix bundle. Clearly, the presence of the expected secondary structure would not prove that the designed tertiary structure was present.

Applicability to Other Systems. In native proteins, cysteine disulfide bonds[38] and proline cis–trans isomerizations[39] play important roles in defining the tertiary structure. Since these isomerizations are slow at room temperature, intermediate protein species can be isolated.[5] Our work on a simple model system suggests that artificial proteins with similar properties can be designed for the study of protein potential energy surfaces. There are three requirements for designing systems with trapped protein states. First, to allow determination of their relative energies, the states must form in or be capable of equilibration to thermodynamic ratios. Second, isomerization must be sufficiently slow to allow separation of the states. Third, there must be a limited number of isomers. Many template-assembled proteins are made by forming covalent bonds (DCC couplings, thiols + acetyl bromides, oximes, reductive amination, etc.). These bonds may be formed under kinetic rather than thermodynamic control, and they are too stable to permit equilibration of protein states. Examples of bonds formed under thermodynamic control include Schiff base formation, some kinds of metal coordination, the cis–trans isomerism of proline amide bonds, and disulfide formation. An alternate template which might produce metastable protein states is tetraphenyl porphyrin, in which the phenyl groups rotate[40] and could carry an attached helix from one face of the porphyrin to the other.

Conclusions

The presence of metastable states in this template-assembled protein has allowed us to study the potential energy surface of the protein moiety in $Fe(pepy)_3$ in an unusual amount of detail. In the region of conformational space that we can see with the four iron tris(chelate) templates, the protein resembles a molten globule rather than a folded protein. Four isomeric species of nearly identical energies are formed. The isomeric proteins have moderate to high secondary structure content, yet they tolerate 5-Å displacements of one peptide relative to the other two with only minor energetic consequences. The potential energy surface is surprisingly flat; there are few barriers to motion on that surface that are as large as the energy required to unbundle the helices, and none of the observed barriers are as large as the energy required to unfold the peptides.

It is possible that a good packing arrangement lurks somewhere "off the map"; we are currently trying some modified templates and mutated sequences that will sample different parts of the three-helix bundle conformational space. The equilibrium distribution of the isomers at the metal center is exquisitely sensitive to the relative stabilities of the isomers, which gives us a way to assess the degree of molten globule character as the template and peptide are varied. This approach may be of use to other workers in the field of artifical protein design.

Acknowledgment. This work was supported in part by the donors of the Petroleum Research Fund, administered by the American Chemical Society. M.L. was supported by a fellowship from the Fannie and John Hertz Foundation.

(36) (a) Dawson, P. E.; Kent, S. B. H. *J. Am. Chem. Soc.* **1993**, *115*, 7263–7266, see Figure 1. (b) Osterhout, J. J., Jr.; Handel, T.; Na, G.; Toumadje, A.; Long, R. C.; Connolly, P. J.; Hoch, J. C.; Johnson, W. C., Jr.; Live, D.; Degrado, W. F. *J. Am. Chem. Soc.* **1992**, *114*, 331–337. (c) Mutter, M.; Tuchscherer, G. G.; Miller, C.; Altmann, K.-H.; Carey, R. I.; Wyss, D. F.; Labhardt, A. M.; Rivier, J. E. *J. Am. Chem. Soc.* **1992**, *114*, 1463–1470. (d) Ghadiri, M. R.; Soares, C.; Choi, C. *J. Am. Chem. Soc.* **1992**, *114*, 825–831, see Figure 9. (e) Ghadiri, M. R.; Soares, C.; Choi, C. *J. Am. Chem. Soc.* **1992**, *114*, 4000–4002, see Figure 1. (f) Lieberman, M.; Sasaki, T. *J. Am. Chem. Soc.* **1991**, *113*, 1470–1471, see Figure 1. (g) Hecht, M.; Richardson, J. S.; Richardson, D. C.; Ogden, R. C. *Science* **1990**, *249*, 884–891. (h) Hahn, K. W.; Klis, W. A.; Stewart, J. M. *Science* **1990**, *248*, 1544–1547, see Figures 1 and 2. (i) Ho, S. P.; DeGrado, W. F. *J. Am. Chem. Soc.* **1987**, *109*, 6751–6758.

(37) Harbury et al. report an intriguing system in which mutant leucine zipper peptides displayed multiple aggregation states, allowing separation of protein substates by gel filtration chromatography. However, no thermodynamic information is reported: Harbury, P. B.; Zhang, T.; Kim, P. S.; Alber, T. *Science* **1993**, *262*, 1401–1407. Suckau et al. used electrospray mass spectroscopy to observe multiple stable conformations of cytochrome *c* and RNAse A as gaseous ions: Suckau, D.; Shi, Y.; Beu, S. C.; Senko, M. W.; Quinn, J. P.; Wampler, F. M., III; McLafferty, F. W. *Proc. Natl. Acad. Sci. U.S.A.* **1993**, *90*, 790–793.

(38) (a) Rosenfeld, R. D.; Noone, N. M.; Lauren, S. L.; Rohde, M. F.; Narhi, L. O.; Arakawa, T. *J. Protein Chem.* **1993**, 247–254. (b) Creighton, T. E. *Proteins: Structures and Molecular Principles*; Freeman: New York, 1984; pp 305–311.

(39) (a) Semisotnov, G. V.; Uversky, V. N.; Sokolovsky, I. V.; Gutin, A. M.; Razgulyaev, O. I.; Rodionova, N. A. *J. Mol. Biol.* **1990**, *213*, 561–568. (b) Kim, P. S.; Baldwin, R. L. *Ann. Rev. Biochem.* **1982**, *51*, 459–489.

(40) Mihara, H. Personal communication, Nagasaki University, 1993.